

Integrative analysis of ferroptosis regulators for clinical prognosis based on deep learning and potential chemotherapy sensitivity of prostate cancer

Tuanjie Guo^{1,§}, Zhihao Yuan^{1,§}, Tao Wang¹, Jian Zhang¹, Heting Tang¹, Ning Zhang^{2,*}, Xiang Wang^{1,*} and Siteng Chen^{3,*}

¹Department of Urology, Shanghai General Hospital, Shanghai Jiao Tong University School of Medicine, Shanghai 200080, China

²Department of Urology, Ruijin Hospital, Shanghai Jiao Tong University School of Medicine, Shanghai 200025, China

³Department of Urology, Renji Hospital, Shanghai Jiao Tong University School of Medicine, Shanghai 200001, China

*Correspondence: Ning Zhang, zn12235@rjh.com.cn; Xiang Wang, seanw_hs@163.com; Siteng Chen, siteng@sjtu.edu.cn

§Tuanjie Guo and Zhihao Yuan contributed equally to this work.

Abstract

Exploring useful prognostic markers and developing a robust prognostic model for patients with prostate cancer are crucial for clinical practice. We applied a deep learning algorithm to construct a prognostic model and proposed the deep learning-based ferroptosis score (DLF_{score}) for the prediction of prognosis and potential chemotherapy sensitivity in prostate cancer. Based on this prognostic model, there was a statistically significant difference in the disease-free survival probability between patients with high and low DLF_{score} in the The Cancer Genome Atlas (TCGA) cohort ($P < 0.0001$). In the validation cohort GSE116918, we also observed a consistent conclusion with the training set ($P = 0.02$). Additionally, functional enrichment analysis showed that DNA repair, RNA splicing signaling, organelle assembly, and regulation of centrosome cycle pathways might regulate prostate cancer through ferroptosis. Meanwhile, the prognostic model we constructed also had application value in predicting drug sensitivity. We predicted some potential drugs for the treatment of prostate cancer through AutoDock, which could potentially be used for prostate cancer treatment.

Keywords: ferroptosis, prostate cancer, deep learning, prognosis, drug sensitivity

Introduction

Prostate cancer is a malignant tumor that affects millions of men around the world, and patients are concentrated mainly in relatively developed regions.¹ More than 1.2 million new cases are diagnosed each year, and prostate cancer-related deaths exceed 350 000 worldwide, making it one of the leading causes of cancer-related deaths.^{1,2} In addition, prostate cancer is the second most common cancer in men and accounts for 7% of new cancer diagnoses in males worldwide. Since the prognosis of patients with prostate cancer is highly variable, doctors mainly depend on tumor grade and stage to predict the prognosis of patients. Although several biomarkers have been reported to predict the prognosis of prostate cancer patients, few of them could finally be used in clinical practice.³

Ferroptosis is a kind of programmed cell death mode caused by intracellular lipid peroxidation and the accumulation of reactive oxygen species of lipids, which is widely studied and provides new ideas for cancer treatment.⁴ Ghoochani *et al.* have found that ferroptosis induction could be used as a new treatment strategy for advanced prostate cancer by single therapy or in combination with second-generation anti-androgen therapy.⁴ Furthermore, some researchers have found that the hyperactive mutation of phosphoinositide 3-kinase protein kinase B-mammalian target of rapamycin (phosphoinositide 3-kinase (PI3K)-AKT-mTOR) signaling protects cancer cells from oxidative stress and ferroptosis through sterol regulatory element binding factor 1/steroloyl

CoA desaturase 1 (SREBP1/SCD-1)-mediated adipogenesis.⁵ At present, the prognostic models based on ferroptosis-related genes mainly depend on the least absolute shrinkage and selection operator (LASSO) Cox regression model, with notable shortcomings of low accuracy and low application value.^{6,7} A neural network-based deep learning analysis of ferroptosis regulators for clinical prognosis in prostate cancer has not been reported yet.

In this study, we used ferroptosis-related genes as raw material and used deep learning algorithms to construct a prognostic model for patients with prostate cancer. We verified the robustness of the prognostic model and analyzed the possible biological mechanisms involved in the prediction of targeted drugs.

Materials and methods

Patient cohorts and data sources

Two patient cohorts with prostate cancer were included in this study: The Cancer Genome Atlas (TCGA, <https://portal.gdc.cancer.gov/>) cohort and the GSE116918 (<https://www.ncbi.nlm.nih.gov/geo/>) cohort.⁸ Only patients with complete gene expression data and clinical information were included in the study. In total, 491 patients with prostate cancer were included in the TCGA cohort, and their mRNA sequencing data and the corresponding clinical information were downloaded from the TCGA database. In the GSE116918 cohort, a total of 248 prostate cancer patients with mRNA sequencing data and corresponding clinical informa-

Received: December 16, 2022. Accepted: January 31, 2023. Published: 2 February, 2023

© The Author(s) 2023. Published by Oxford University Press on behalf of the West China School of Medicine & West China Hospital of Sichuan University. This is an Open Access article distributed under the terms of the Creative Commons Attribution-NonCommercial License (<https://creativecommons.org/licenses/by-nc/4.0/>), which permits non-commercial re-use, distribution, and reproduction in any medium, provided the original work is properly cited. For commercial re-use, please contact journals.permissions@oup.com

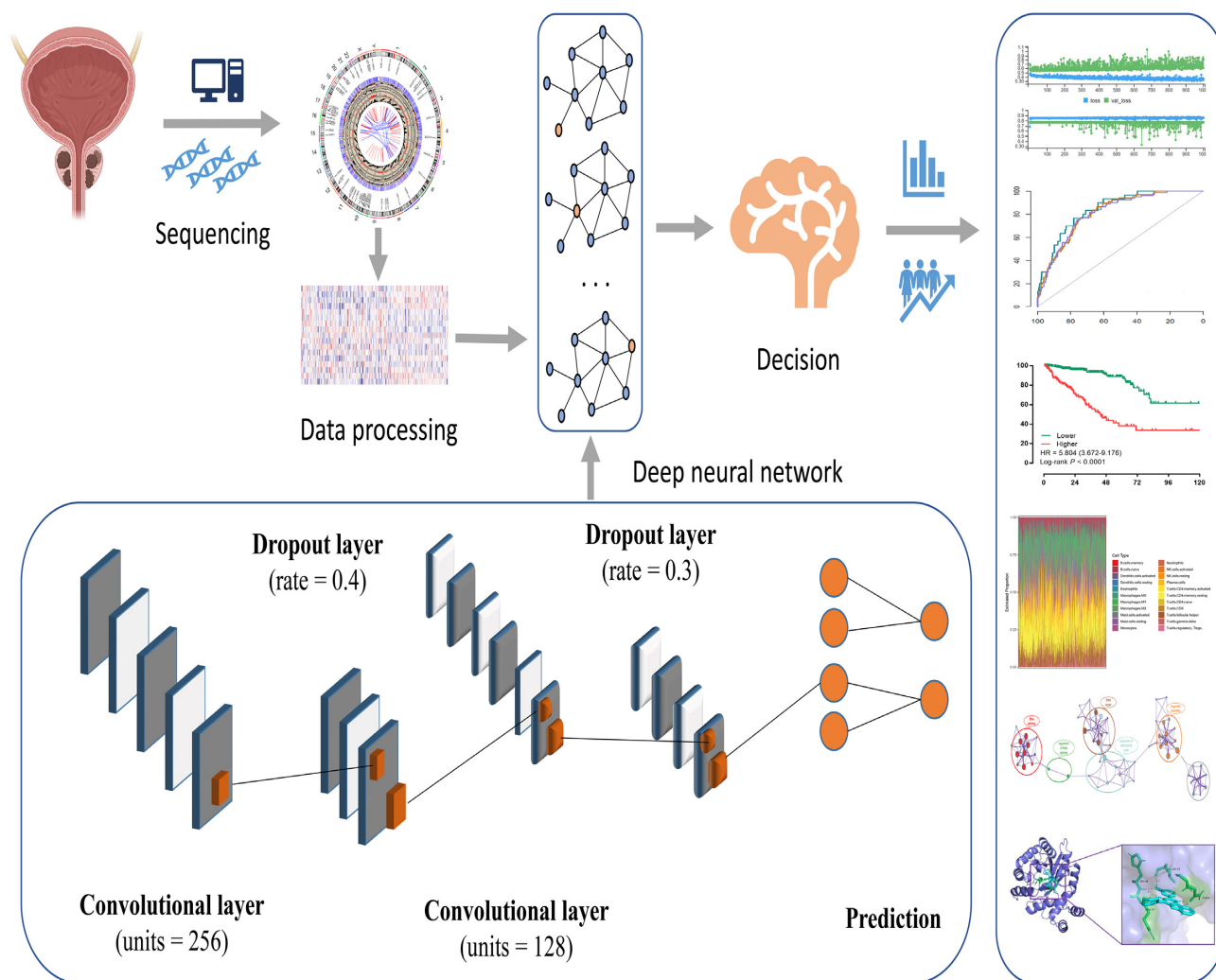


Figure 1. The workflow of this study.

tion were recruited from the Gene Expression Omnibus (GEO) database. The basic clinical characteristics of the included patients are described in Table S1, see online supplementary material. We also included a cohort of pan-cancer patients of 32 malignancies, including normalized RNA-seq data and survival information from 10 144 patients. Simultaneously, we recruited ferroptosis-related genes according to previous studies,^{9,10} which had been proved to be valid candidates for the prediction of clinical prognosis of malignant tumors. After eliminating genes with very low expression in prostate cancer, 54 ferroptosis-related genes were finally selected for further analysis (Table S2, see online supplementary material).

Prognostic model construction based on deep learning

The network framework of the deep learning algorithm is shown in Fig. 1, and was developed based on a high-level neural network (<https://keras.rstudio.com>) with Tensorflow. The prediction model was defined using the sequential application programming interface. There were three dense layers with a rectified linear unit activation function in the framework. For the first dense layer with units of 256 and activation of the rectified linear unit, the input tensor was defined as 54, since the input file contained the expression of 54 ferroptosis-related genes. A dropping rate of 0.4 was set for the first dropout layer. The second dense layer was defined

with units of 128 and activation of the rectified linear unit, which was followed by the second dropout layer with a dropping rate of 0.3. The loss function was set as a sparse categorical cross-entropy, with an optimizer of RMSprop and metrics of accuracy according to our previous study.¹¹ In the third dense layer (the output layer), the output result was directly taken as the deep learning-based ferroptosis score (DLF_{score}). 54 ferroptosis-related core genes were included in the calculation of DLF_{score}. The output result was calculated via superimposed calculation of the predicted value according to the weight coefficient and expression value of each gene.

Cox regression analysis and survival analysis

Cox regression analysis was implemented through the dplyr and survival packages. The survival analysis in this study was implemented through survival and survminer packages. Data visualization was achieved through the ggplot2 package. The analysis process and visualization were completed in the R environment.

Analysis of tumor immune microenvironments

The CIBERSORT algorithm was applied to evaluate the landscape of immune cells and the difference of immune cell infiltration. The settings of specific parameters can be found in our previously published article.¹²

Functional enrichment analysis

To explore the possible mechanism related to the DLF_{score} and prognosis, we used weighted gene co-expression network analysis (WGCNA) based on differentially expressed genes ($|\text{fold change}| \geq 1$, $P < 0.05$) in prostate cancer patients.¹³ Correlation analysis was performed to find the best module that was most relevant to the DLF_{score} . Finally, using the Kyoto Encyclopedia of Genes and Genomes (KEGG) and genetic ontology (GO) analysis, we explored the potential biological mechanisms of ferroptosis-related genes that could participate in Metascape.¹⁴

Exploration of potential drugs and semiflexible docking analysis

The 13 potential drug targets and their RNA composite expression data were obtained from the CellMiner database (<https://discover.nci.nih.gov/cellminer/home.do>). Association analysis of ferroptosis regulator RNA complex expression was performed using the mean compound activity z score (DTP NCI-60). AutoDock Vina software was used for semi-flexible docking to study the interaction between PI-103 and ferroptosis regulatory factors such as AKRIC3.¹⁵ The 3D structure information of the AKRIC3 protein was obtained from the PubChem database (<https://pubchem.ncbi.nlm.nih.gov>). In docking analysis, PI-103 was flexible and the protein was rigid. When using AutoDock Vina for docking, the entire protein surface served as AKRIC3 binding targets. Finally, we visually docked the model with PyMOL.¹⁶

Construction of a predictive nomogram based on DLF_{score}

To conveniently and intuitively predict patient outcomes, we constructed a predictive nomogram model combining the DLF_{score} and the clinicopathological characteristics of the patients. The method of constructing the nomogram is available in our previous research.^{12,17}

Statistical analysis

In this study, we used the Mann–Whitney U test to analyze the difference between continuous variables and the Analysis of Variance (ANOVA) test for continuous variables of more than two groups. Kaplan–Meier curve analysis was used to compare disease-free survival (DFS) with the log-rank test. Comparisons between different areas under the curve (AUCs) were performed through a nonparametric approach reported by DeLong et al.¹⁸ All statistical analyses were performed in R (4.0.0) and GraphPad Prism 8.

Results

Development and verification of the deep learning-based prognosis model

The DLF_{score} was obtained by deep learning of 54 ferroptosis-related genes in the TCGA cohort. The AUC values obtained by the receiver operating characteristic (ROC) curve analysis for predicting 1, 3, and 5-year DFS by the prognostic model were 0.843, 0.816, and 0.811, respectively (Fig. 2A). At the same time, we applied the confusion matrix to evaluate the prediction model based on deep learning (Fig. 2B). Meanwhile, we constructed a prognostic model based on LASSO Cox regression, which was significantly less accurate than deep learning in predicting the prognosis (Table S3, see online supplementary material). In the GSE116918 validation cohort, deep learning also showed very good performance in pre-

dicting 3, 5, and 10-year DFS (Fig. S1, see online supplementary material). According to the cutoff value of DLF_{score} (0.1411) in the TCGA cohort, the patients were divided into the high-score group and low-score group. There was a significant difference in the DFS [hazard ratio = 5.804, 95% confidence interval (CI): 3.672–9.176, $P < 0.0001$] between the high-score group and the low-score group (Fig. 2C). Then we validated this model in the GSE116918 cohort (Fig. 2C) with the same cut-off value, and the result showed that the DFS of different score groups also had a strongly significant difference (hazard ratio = 2.597, 95% CI: 1.002–6.599, $P = 0.02$). Collectively, these results suggested that the prognostic model we constructed was strongly correlated with the prognosis of the patient. Further, Cox regression analysis indicated that DLF_{score} could be used as a prognostic factor for prostate cancer patients (Fig. 2D).

Evaluation of the robustness of the prognostic model

The presence of a positive surgical margin was associated with biochemical recurrence-free survival, cancer-specific survival, overall survival, cancer-specific mortality, and overall mortality in patients with prostate cancer.¹⁹ Therefore, we further explored whether the constructed prognostic model could stratify the survival of patients with different surgical margin statuses. We found that in the surgical margin-negative group, patients with high DLF_{score} tended to have a lower probability of DFS, and patients with low DLF_{score} tended to have a higher probability of DFS (Fig. 3A). In the surgical margin-positive group, the DLF_{score} could also distinguish different clinical prognosis between patients with high DLF_{score} and low DLF_{score} (Fig. 3B). These results suggested that the DLF_{score} had a significant stratification effect on the DFS of patients with different surgical margin characteristics. In addition, we found that the DLF_{score} was related to the progress of prostate cancer. With the increase of T stage and Gleason score, the DLF_{score} also increased, which was consistent in the two prostate cancer cohorts (Fig. 3C–F), indicating that the DLF_{score} could reflect the progress of prostate cancer.

Subsequently, we applied the prognostic model to pan-cancer analysis and found that it could also play a prognostic role in a pan-cancer cohort (Fig. 3G). Cox regression analysis showed that DLF_{score} could be used as an independent risk factor for multiple tumors (Fig. 3H). In conclusion, the DLF_{score} had strong robustness and specificity in predicting the prognosis of patients with prostate cancer.

Exploration of immune infiltration characteristics among patients with different DLF_{score}

To explore whether the proportion of immune cells of patients with different scores was different, we carried out an analysis of immune infiltration. We analyzed and evaluated the landscape of various immune cells in the tumor microenvironment in the TCGA cohort (Fig. 4A). We found that the top three cell types in the prostate cancer microenvironment were CD4 memory resting cells, plasma cells, and M2 macrophages (Fig. 4B). In addition, we compared the proportion of various immune cells among patients with different DLF_{score} . Our results revealed that more M2 macrophages, Treg cells, and CD8 T cells were found in patients with higher DLF_{score} (Fig. 4C). Therefore, it is concluded that patients with higher DLF_{score} had more immunosuppressive cells in the tumor microenvironment, which was consistent with a previous study that reported the immunosuppressive function in prostate cancer.¹⁹

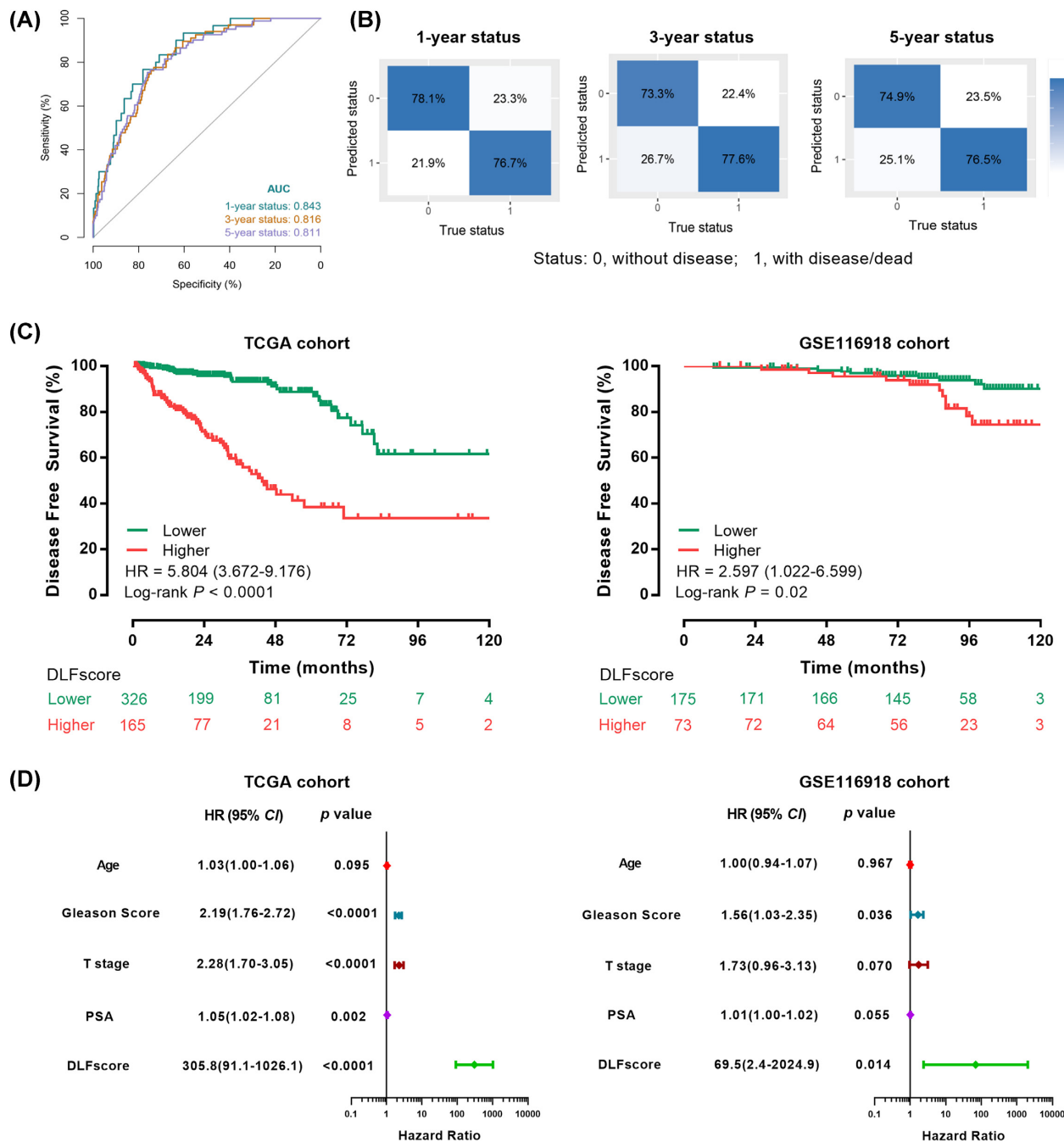


Figure 2. Prognosis model based on ferroptosis-related genes for prostate cancer. (A) Receiver operating characteristic curve analysis of 1-, 3- and 5-year disease-free survival prediction through the prognostic model. (B) Confusion matrices for the evaluation of the deep learning-based prediction model. The profile of coefficients in the model at varying levels of penalization is plotted against the log (λ) sequence. (C) Kaplan–Meier survival analysis of disease-free survival stratified by DLF_{score} for prostate cancer patients in the TCGA cohort and validation GSE116918 cohort, respectively. (D) Univariate Cox regression analysis of DLF_{score} and clinicopathological factors in the TCGA cohort and the GSE116918 validation cohort. TCGA, The Cancer Genome Atlas; AUC, area under curve; DLF_{score}, deep learning-based ferroptosis score.

WGCNA revealed that DLF_{score} is related to DNA repair and RNA splicing

Based on WGCNA, we performed a functional enrichment analysis of differentially expressed genes in prostate cancer patients (Fig. 5A). Firstly, we modularized the enriched genes (Fig. 5B). Subsequently, by associating the modular genes with the clinical characteristics and DLF_{score}, we found that the blue module has the

highest correlation with the DLF_{score} (Fig. 5C). Finally, we analyzed the blue module genes through GO and KEGG, and we found that the enriched genes were related to DNA repair, RNA splicing, organelle assembly, and regulation of the centrosome cycle pathway (Fig. 5D). Collectively, these results demonstrated that ferroptosis-related genes may regulate tumor progression through these signaling pathways.

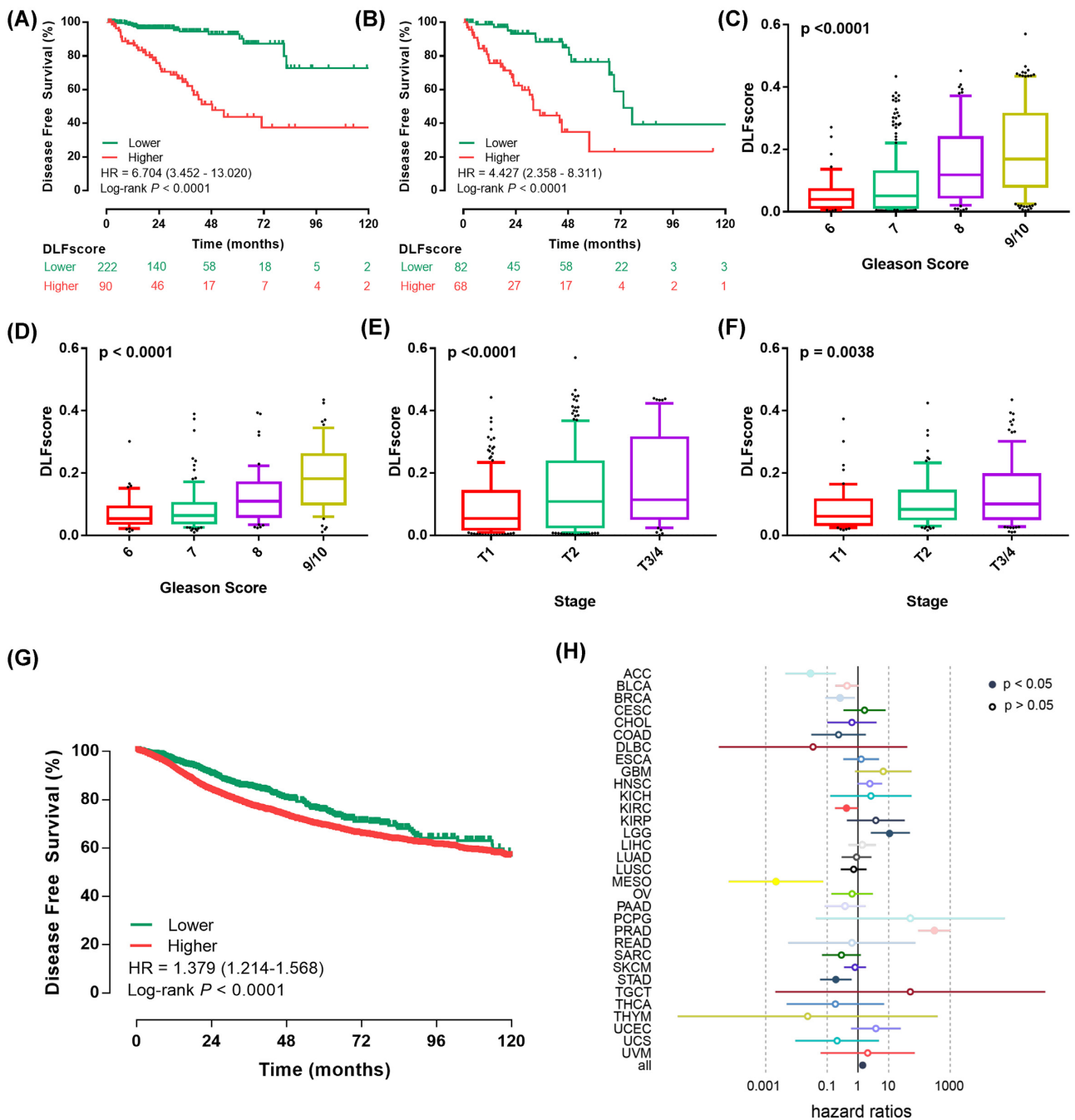


Figure 3. Evaluation of the deep-learning model based on ferroptosis-related genes. Kaplan-Meier survival analysis of disease-free survival stratified by DLF_{score} for prostate cancer patients (A) without and (B) with positive surgical margin in the TCGA cohort. Different distributions of DLF_{score} among patients with different Gleason scores in (C) the TCGA cohort and (D) the GSE116918 cohort. Distribution of DLF_{score} among patients with different tumor stages in (E) the TCGA cohort and (F) the GSE116918 cohort. (G) Kaplan-Meier survival analysis of disease-free survival stratified by DLF_{score} for pan-cancer patients from the TCGA data set. (H) Cox regression analysis of the deep learning-based model in different kinds of malignancies. TCGA, The Cancer Genome Atlas; DLF_{score}, deep learning-based ferroptosis score; HR, hazard ratio.

Prediction of therapeutic drugs regulating ferroptosis based on DLF_{score}

Next, we explored the possibility of applying our prognostic model to the prediction of drugs targeting the regulation of prostate cancer. We found five ferroptosis regulatory genes in two prostate cancer cohorts, and their expression levels were strongly correlated with the DLF_{score} (Fig. 6A). We performed a correlation analysis of drug complex activity and ferroptosis-related gene expression in the NCI 60 cell line (Fig. 6B). We compared the differences

in drug sensitivity among different DLF_{score} in the cell line and found that DLF_{score} could be used to predict the sensitivity of the cell line to drugs, including PI-103, 6-mercaptopurine, fenretinide, curumin, and lapachone (Fig. 6C). We used drug PI-103 and protein AKR1C3 as an example for docking simulation of drug and protein binding sites. Figure 6D shows the 3D structure of PI-103. The molecular docking sites of the PI-103 and AKR1C3 proteins are illustrated in Fig. 6E. The binding energy obtained from the docking of AKR1C3 with PI-103 was -6.74 kcal/mol on Autodock

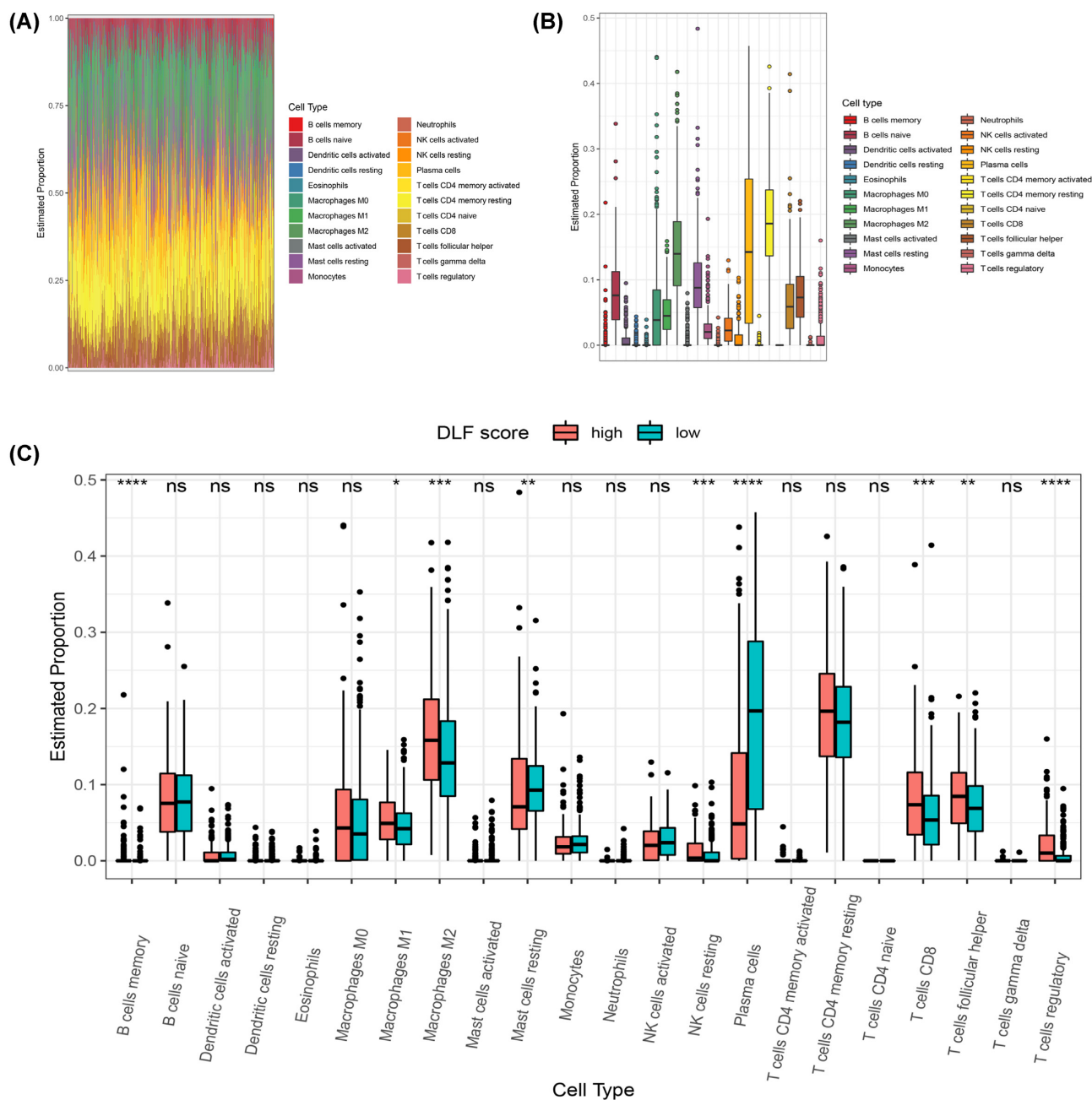


Figure 4. Tumor microenvironment analysis in the TCGA cohort. **(A)** Different immune cells in the tumor microenvironment. **(B)** Different abundances of each immune cell types in prostate cancer. **(C)** The difference in the proportion of immune cells between the high-score group and the low-score group. TCGA, the cancer genome atlas; DLF_{score} , deep learning-based ferroptosis score; HR, hazard ratio. * $P < 0.05$; ** $P < 0.01$; *** $P < 0.001$; **** $P < 0.0001$; ns: no significance.

Vina. Together, these results revealed a critical role of DLF_{score} in drug sensitivity prediction.

Construction of a nomogram based on DLF_{score} for prostate cancer patients

To apply our prognostic model to predict the survival time of prostate cancer patients, we constructed a nomogram prognostic model (Fig. 7A). Through the nomogram, we could intuitively predict the DFS probability of patients for 1-, 3- and 5-years. The calibration analysis indicated that the survival rate predicted by the nomogram had excellent agreement with actual observations at 1-, 3- and 5-year follow up (Fig. 7B). ROC curve analyses illus-

trated that the AUCs of the nomogram for survival prediction of 1-, 3- and 5-years reached 0.84, 0.86, and 0.90, respectively (Fig. 7C). When our model was combined with clinicopathological information, the accuracy of patient prognosis prediction was significantly improved. These results further confirmed the role of DLF_{score} in predicting the survival of prostate cancer patients.

Discussion

Currently, ~700 000 patients may be subjected to metastatic prostate cancer, which causes >400 000 deaths each year.^{20,21} Given the high incidence and mortality of prostate cancer, it is

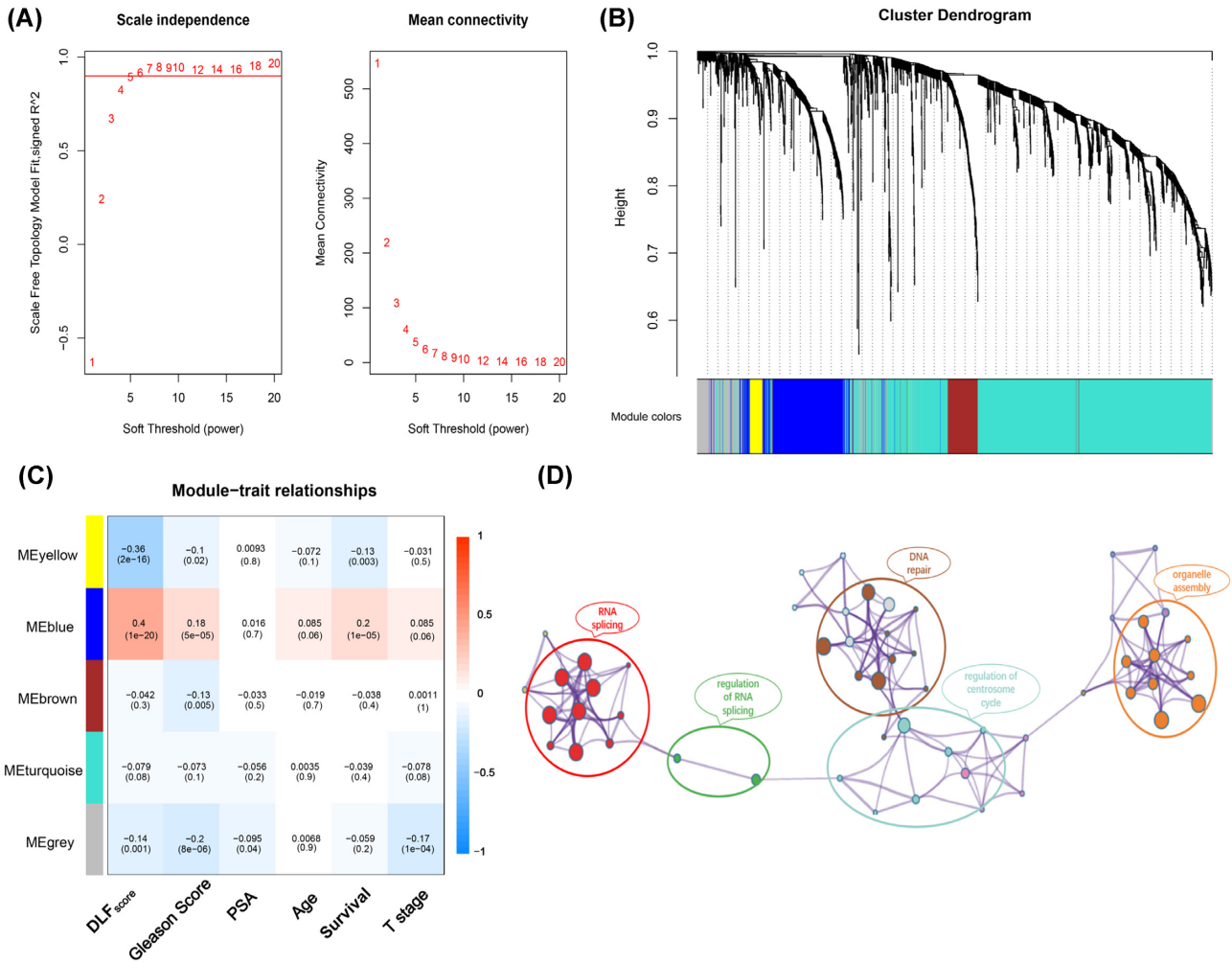


Figure 5. WGCNA for differentially expressed genes between high and low DLF_{score} groups in prostate cancer. **(A)** Soft power estimation in prostate cancer for WGCNA. **(B)** Gene dendrogram with different colors showing the modules identified by WGCNA. **(C)** The relationship between gene modules and clinical characteristics. **(D)** Potentially enriched pathways of the co-expressed genes in the blue module. WGCNA, weighted gene co-expression network analysis; DLF_{score}, deep learning-based ferroptosis score.

extremely important to develop prognostic models for patients with prostate cancer. In addition, current prognostic models based on simple machine-learning methods may be restricted by their drawbacks of unsatisfied accuracy and limited application value.

In this study, we performed a deep learning-based integrative analysis of ferroptosis regulators for clinical prognosis of patients with prostate cancer. Our previous study preliminarily proved the superiority of the deep learning-based prognostic model over the LASSO-based method.¹¹ In this study, the AUC value of the deep learning-based prognostic model was significantly higher than that of the LASSO-based prognostic model.^{6,7} The model we constructed could effectively stratify the survival probability of patients. We also found that DLF_{score} could be a useful prognostic factor for prostate cancer.

Traditional tumor node metastasis (TNM) staging for predicting the prognosis is limited to the macroscopic characteristics of the tumor, and its prediction of the prognosis does not meet the precision requirement for individuals. Prostate-specific antigen (PSA) is influenced by many factors, and it is also very unstable in predicting prognosis. Deep learning-based prognostic models are significantly more effective than traditional TNM, Gleason score, and PSA (Fig. 2D). Apart from that, the prognostic model

based on deep-learning algorithms is more robust than other traditional machine-learning algorithms in terms of predicting prognostic accuracy.¹¹ It fully takes into account the intrinsic connection between all genes. However, the disadvantages of deep learning are obvious, such as the large amount of data required and the complexity of the algorithm, which makes clinical application relatively complicated.

The development of prostate cancer is associated with acquired somatic genetic alterations and complex interactions in the microenvironment. Some studies have pointed out that chronic inflammation and infection drive the occurrence of prostate cancer through the production of oxidative stress and reactive oxygen species, inducing DNA damage and the selection of mutant cells.²² DNA damage response genes also play key roles in prostate cancer. Men with germline mutations in BRCA1 or BRCA2 had higher risk of prostate cancer.²³ Prostate cancer patients with germ cell mutations in BRCA2 tended to have worse clinical outcomes.²⁴ Approximately 23% of metastatic prostate cancers developed somatic aberrations in DNA damage response genes.²⁵ Radiation therapy is widely used to treat cancer, and resistance mechanisms often involve activation of DNA repair and inhibition of apoptosis. In models of human-patient-derived lung adenocarcinoma and glioma,

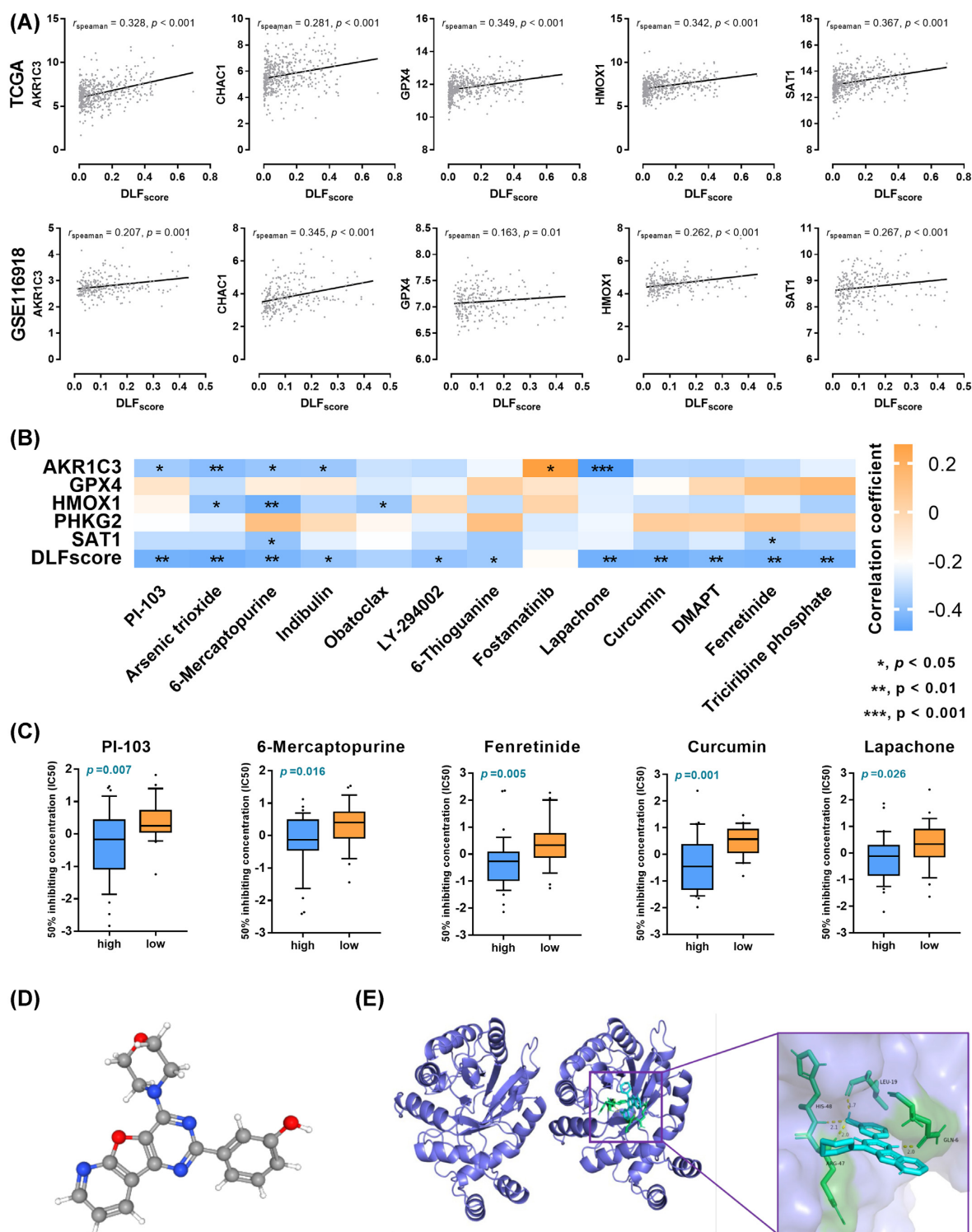


Figure 6. Prediction of therapeutic agents for use in ferroptosis regulation. (A) Correlation analysis of DLF_{score} and ferroptosis-related gene expression. (B) Correlation analysis of the compound activity of drugs and ferroptosis-related genes and DLF_{score} in the NCI 60 cell line. (C) Comparison of drug sensitivity between prostate cancer cell lines with high and low DLF_{score} . (D) The molecular structure of PI-103. (E) The docking result of the active components to AKR1C3. Diagram of the cyclophosphamide and protein combination. IC50, half-maximal inhibitory concentration; * $P < 0.05$; ** $P < 0.01$; DLF_{score} , deep learning-based ferroptosis score.

ferroptosis inducer could enhance the antitumor effects of radiation.²⁶ Another study found that radiotherapy-induced ferroptosis and increased ferroptosis in patients were associated with a better response to radiotherapy and longer clinical survival.²⁷ In this study, we found that the ferroptosis-related prognostic model

was mainly related to the DNA repair signaling pathway. Therefore, whether ferroptosis was a programmed response after DNA damage deserves further study.

Few studies focused on the relationship between ferroptosis and the regulation of the centrosome cycle. However, a recent

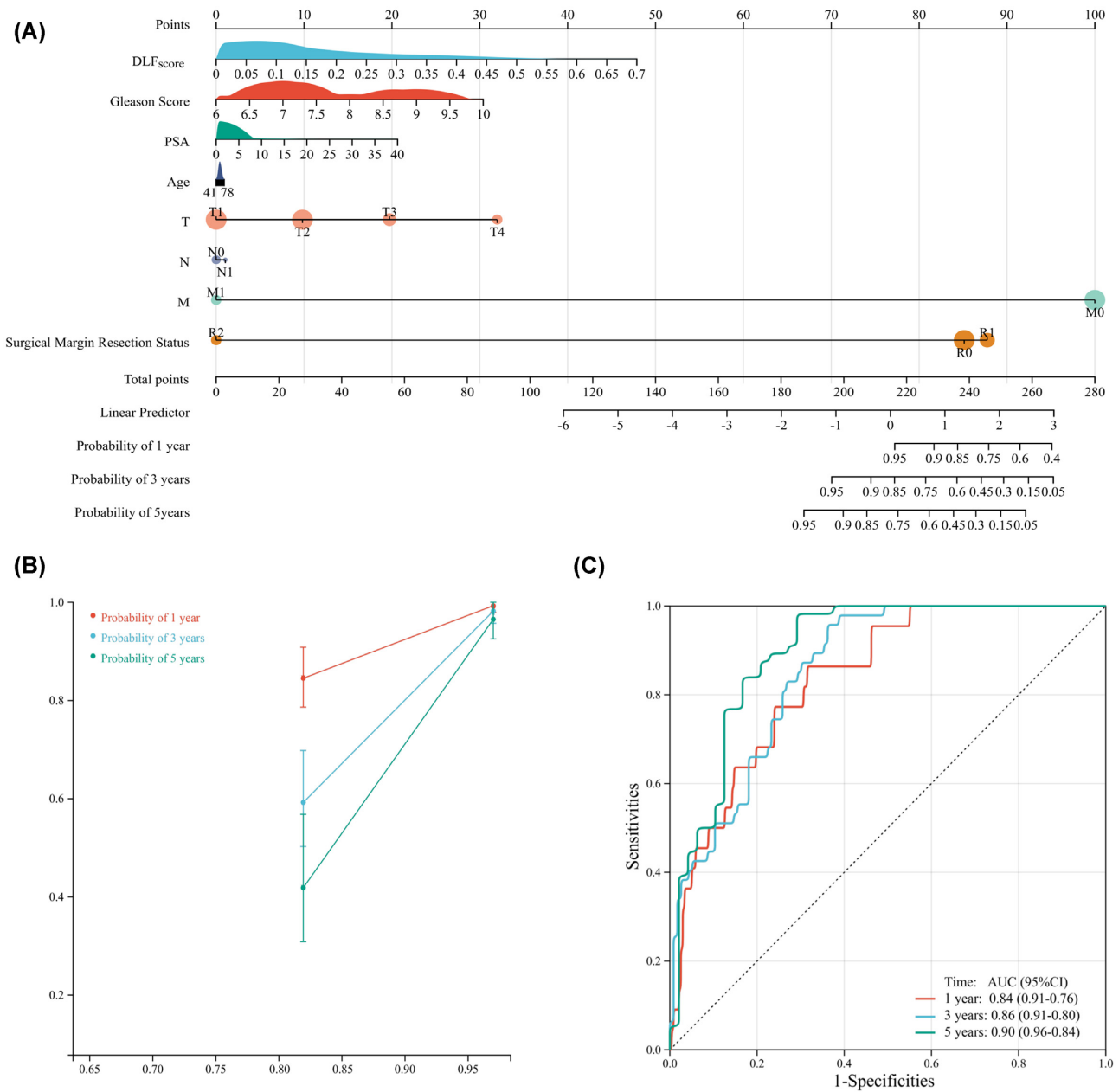


Figure 7. Construction and evaluation of a nomogram prognosis model in the TCGA cohort. **(A)** Nomogram based on DLF_{score} and clinicopathological factors for 1-, 3- and 5-year disease-free survival prediction of prostate cancer patients. **(B)** Evolution of the prognostic nomogram model for 1-, 3- and 5-year disease-free survival prediction. **(C)** ROC curve of 1-, 3- and 5-year disease-free survival prediction for the prognostic nomogram model. TCGA, The cancer genome atlas; DLF_{score}, deep learning-based ferroptosis score; ROC, receiver operating characteristic; AUC, area under the curve; PSA, prostate-specific antigen.

study found that centrosome protein 290 was a new prognostic marker that regulated ferroptosis in liver cancer cells through the nuclear factor erythroid 2-related factor 2 (Nrf2) pathway.²⁸ Studies of ferroptosis and RNA splicing have also rarely been reported; only the RNA-binding protein NF-kappaB activating protein (NKAP) was found to protect glioblastoma cells from ferroptosis by promoting N6-methyladenosine (m6A)-dependent splicing of SLC7A11 mRNA.²⁹ Research on ferroptosis and organelle assembly was a gap that needed to be filled in the field of scientific research. Therefore, the relationship between ferroptosis and organelle assembly, regulation of centrosome cycle, and RNA splicing needed to be further studied. In this study, we identified a close relationship between ferroptosis and DNA repair, RNA splic-

ing signaling, organelle assembly, and regulation of centrosome cycle pathways, which was a conclusion worthy of attention.

Some studies had found that AKR1C3 activation was a key resistance mechanism associated with resistance to enzalutamide. Targeting endogenous androgens and AKR1C3 could overcome enzalutamide resistance and improve the survival rate of patients with advanced prostate cancer.²⁶ Recently, a compound named MF-15 was found to have strong effects on androgen receptor (AR) signaling, including significant inhibition of AR activity, downregulation of androgen-regulated genes, and reduction of PSA production, reducing AR and AKR1C3 expression. However, the specific mechanism is still unclear.³⁰ PI-103 is a PI3K inhibitor that can induce apoptosis, reduce autophagy, and in-

hibit the PI3K/Akt/mTOR pathway. However, its inhibitory effect on AKR1C3 had not yet been reported.^{28,29} Our study found that PI-103 might be a drug targeting AKR1C3, which also indicated that PI-103 might be a potential drug for the treatment of prostate cancer.

This study still had some limitations. First of all, the study conducted cross-validation of two independent prostate cancer cohorts and a pan-cancer cohort, but there might still be potential bias due to the use of retrospective cohort analysis. Second, prospective single-center or multicenter studies are still needed to further verify the robustness of the prognosis model. Finally, although our study revealed that DNA repair, RNA splicing, organelle assembly, and regulation of centrosome cycle pathways were associated with DLF_{score} in prostate cancer, the exploration of potential mechanisms and functional verification of experimental studies remain to be performed.

Conclusions

We constructed a prognostic model for prostate cancer patients using ferroptosis-related genes based on a deep-learning algorithm. In addition, we constructed a predictive nomogram for prostate cancer patients based on DLF_{score} and clinicopathological features. The enrichment analysis found that DLF_{score} was associated with DNA repair, RNA splicing signaling, organelle assembly, and regulation of centrosome cycle pathways. More importantly, the prognostic model we constructed also has application value in predicting drug sensitivity.

Supplementary data

Supplementary data is available at [PCMED](#) online.

Acknowledgments

This work was supported by the National Natural Science Foundation of China (Grant No. 82172920).

Conflict of interest

None declared.

Author contributions

X.W., N.Z., and S.C. designed the experiments. T.G. and Z.Y. carried out experiments and wrote the manuscript. J.Z., T.W., and H.T. performed the manuscript review and data analysis. All authors contributed to the article and approved the submitted version.

Data availability

The raw data used in this study may be downloaded from the TCGA (<https://portal.gdc.cancer.gov/>) and GSE116918 databases (<https://www.ncbi.nlm.nih.gov/geo>).

References

- Rebello RJ, Oing C, Knudsen KE, et al. Prostate cancer. *Nat Rev Dis Primers* 2021;**7**:9. doi: 10.1038/s41572-020-00243-0.
- Bray F, Ferlay J, Soerjomataram I, et al. Global cancer statistics 2018: GLOBOCAN estimates of incidence and mortality worldwide for 36 cancers in 185 countries. *CA Cancer J Clin* 2018;**68**:394–424. doi: 10.3322/caac.21492.
- Cucchiara V, Cooperberg MR, Dall'Era M, et al. Genomic markers in prostate cancer decision making. *Eur Urol* 2018;**73**:572–82. doi: 10.1016/j.eururo.2017.10.036.
- Ghoochani A, Hsu E-C, Aslan M, et al. Ferroptosis Inducers Are a Novel Therapeutic Approach for Advanced Prostate Cancer. *Cancer Res* 2021;**81**(6): 1583–1594. PMID: 33483372 PMID: PMC7969452. doi: 10.1158/0008-5472.CAN-20-3477.
- Yi J, Zhu J, Wu J, et al. Oncogenic activation of PI3K-AKT-mTOR signaling suppresses ferroptosis via SREBP-mediated lipogenesis. *Proc Natl Acad Sci* 2020;**117**:31189–97. doi: 10.1073/pnas.2017152117.
- Liu H, Gao L, Xie T, et al. Identification and validation of a prognostic signature for prostate cancer based on ferroptosis-related genes. *Front Oncol* 2021;**11**:623313. doi: 10.3389/fonc.2021.623313.
- Ke Z-B, You Q, Sun J-B, et al. A novel ferroptosis-based molecular signature associated with biochemical recurrence-free survival and tumor immune microenvironment of prostate cancer. *Front Cell Dev Biol* 2021;**9**:774625. doi: 10.3389/fcell.2021.774625.
- Long Q, Xu J, Osunkoya AO, et al. Global transcriptome analysis of formalin-fixed prostate cancer specimens identifies biomarkers of disease recurrence. *Cancer Res* 2014;**74**:3228–37. doi: 10.1158/0008-5472.CAN-13-2699.
- Liang JY, Wang DS, Lin HC, et al. A novel ferroptosis-related gene signature for overall survival prediction in patients with hepatocellular carcinoma. *Int J Biol Sci* 2020;**16**:2430–41. doi: 10.7150/ijbs.45050.
- Tang B, Yan R, Zhu J, et al. Integrative analysis of the molecular mechanisms, immunological features and immunotherapy response of ferroptosis regulators across 33 cancer types. *Int J Biol Sci* 2022;**18**:180–98. doi: 10.7150/ijbs.64654.
- Chen S, Zhang E, Jiang L, et al. Robust prediction of prognosis and immunotherapeutic response for clear cell renal cell carcinoma through deep learning algorithm. *Front Immunol* 2022;**13**:798471. doi: 10.3389/fimmu.2022.798471.
- Guo T, Zhang J, Wang T, et al. Lactic acid metabolism and transporter related three genes predict the prognosis of patients with clear cell renal cell carcinoma. *Genes (Basel)* 2022;**13**:620. doi: 10.3390/genes13040620.
- Tang Z, Kang B, Li C, et al. GEPIA2: an enhanced web server for large-scale expression profiling and interactive analysis. *Nucleic Acids Res* 2019;**47**:W556–60. doi: 10.1093/nar/gkz430.
- Zhou Y, Zhou B, Pache L, et al. Metascape provides a biologist-oriented resource for the analysis of systems-level datasets. *Nat Commun* 2019;**10**:1523. doi: 10.1038/s41467-019-09234-6.
- Trott O, Olson AJ. AutoDock Vina: improving the speed and accuracy of docking with a new scoring function, efficient optimization, and multithreading. *J Comput Chem* 2010;**31**:455–61. doi: 10.1002/jcc.21334.
- Seeliger D, de Groot BL. Ligand docking and binding site analysis with PyMOL and Autodock/Vina. *J Comput-Aided Mol Des* 2010;**24**:417–22. doi: 10.1007/s10822-010-9352-6.
- Chen S, Zhang E, Guo T, et al. A novel ferroptosis-related gene signature associated with cell cycle for prognosis prediction in patients with clear cell renal cell carcinoma. *BMC Cancer* 2022;**22**:1. doi: 10.1186/s12885-021-09033-7.
- DeLong ER, DeLong DM, Clarke-Pearson DL. Comparing the areas under two or more correlated receiver operating characteristic curves: a nonparametric approach. *Biometrics* 1988;**44**:837–45.
- Tsaur I, Brandt MP, Juengel E, et al. Immunotherapy in prostate cancer: new horizon of hurdles and hopes. *World J Urol* 2021;**39**:1387–403. doi: 10.1007/s00345-020-03497-1.
- Foreman KJ, Marquez N, Dolgert A, et al. Forecasting life expectancy, years of life lost, and all-cause and cause-specific mor-

- tality for 250 causes of death: reference and alternative scenarios for 2016-40 for 195 countries and territories. *Lancet (London, England)* 2018;**392**:2052–90. doi: 10.1016/S0140-6736(18)31694-5.
- 21 Sandhu S, Moore CM, Chiong E, et al. Prostate cancer. *Lancet* 2021;**398**:1075–90. doi: 10.1016/S0140-6736(21)00950-8.
- 22 Sfanos KS, Yegnasubramanian S, Nelson WG, et al. The inflammatory microenvironment and microbiome in prostate cancer development. *Nature Reviews Urology* 2018;**15**:11–24. doi: 10.1038/nrrol.2017.167.
- 23 Taylor RA, Fraser M, Rebello RJ, et al. The influence of BRCA2 mutation on localized prostate cancer. *Nature Reviews Urology* 2019;**16**:281–90. doi: 10.1038/s41585-019-0164-8.
- 24 Castro E, Goh C, Olmos D, et al. Germline BRCA mutations are associated with higher risk of nodal involvement, distant metastasis, and poor survival outcomes in prostate cancer. *Journal of Clinical Oncology: Official Journal of the American Society of Clinical Oncology* 2013;**31**:1748–57. doi: 10.1200/JCO.2012.43.1882.
- 25 Robinson D, Van Allen EM, Wu Y-M, et al. Integrative clinical genomics of advanced prostate cancer. *Cell* 2015;**161**:1215–28. doi: 10.1016/j.cell.2015.05.001.
- 26 Liu C, Lou W, Zhu Y, et al. Intracrine androgens and AKR1C3 activation confer resistance to enzalutamide in prostate cancer. *Cancer Res* 2015;**75**:1413–22. doi: 10.1158/0008-5472.CAN-14-3080.
- 27 Lei G, Zhang Y, Koppula P, et al. The role of ferroptosis in ionizing radiation-induced cell death and tumor suppression. *Cell Res* 2020;**30**:146–62. doi: 10.1038/s41422-019-0263-3.
- 28 Mazzeletti M, Bortolin F, Brunelli L, et al. Combination of PI3K/mTOR inhibitors: antitumor activity and molecular correlates. *Cancer Res* 2011;**71**:4573–84. doi: 10.1158/0008-5472.CAN-10-4322.
- 29 Chang L, Graham PH, Hao J, et al. PI3K/Akt/mTOR pathway inhibitors enhance radiosensitivity in radioresistant prostate cancer cells through inducing apoptosis, reducing autophagy, suppressing NHEJ and HR repair pathways. *Cell Death Dis* 2014;**5**:e1437. doi: 10.1038/cddis.2014.415.
- 30 Kafka M, Mayr F, Temml V, et al. Dual inhibitory action of a novel AKR1C3 inhibitor on both full-length AR and the variant AR-V7 in enzalutamide resistant metastatic castration resistant prostate cancer. *Cancers* 2020;**12**:2092. doi: 10.3390/cancers12082092.